

Electronic Tracking System for Multiplexed Fibre Grating Sensors

H. Geiger, M. G. Xu, N. C. Eaton, J. P. Dakin

Abstract: We demonstrate for the first time an electronic lock-in system using an acousto-optic tunable filter (AOTF) to track the wavelength of a fibre Bragg grating. The system has an output frequency proportional to the grating wavelength. Initial results show microstrain resolution at data acquisition rates of 10 Hz.

Introduction: Since the initial demonstration of Bragg gratings, there has been much interest in their use as sensors for strain and/or temperature [1]. We proposed earlier a lock-in system using an AOTF and showed its viability in open-loop operation monitoring the temperature of a Bragg grating [2]. References to alternative interrogation techniques were also given in this earlier paper.

We report here on design and initial results of the closed-loop system that allows real-time tracking of strain or temperature (Fig. 1).

Interrogation Technique: Light from a broadband source (ELED) illuminates one or more gratings at different Bragg wavelengths through a coupler. The reflected light is filtered by an AOTF and detected by a transimpedance receiver.

The fiber-pigtailed AOTF acts as an optical bandpass filter. Its centre wavelength depends linearly on the RF frequency applied to its electrical input by a voltage-controlled oscillator (VCO).

The interrogation system allows two modes of interrogation: (i) a scan mode and (ii) a lock-in mode. In the scan mode, the feedback loop is disabled and the personal computer (PC) tunes the AOTF via the VCO over the wavelength range of interest. The power reflected from the gratings is recorded. The recorded signal is the correlation between the sum of the gratings' spectra and the AOTF's spectrum in the wavelength domain.

In the lock-in mode, the system tracks the wavelength of a particular grating using the feedback loop. The PC initiates a frequency-shift keying (FSK) of the RF signal to the AOTF by driving the VCO with a square wave. This toggles the centre wavelength of the AOTF between two wavelengths within the bandwidth of a selected grating. When the reflected optical power at these two wavelengths is not equal, the detected optical signal is amplitude-modulated at the toggling frequency. Multiplying the detected signal with the toggling signal generates an error signal proportional to the difference between the mean AOTF wavelength and the grating wavelength. This error signal is integrated and tunes the mean AOTF wavelength to match the grating wavelength. Counting cycles of the AOTF drive signal over integer multiples of the toggling period measures the mean AOTF frequency. The mean frequency gives an accurate measurement of changes in the grating wavelength.

The measurement resolution improves when the gating time of the counter is increased. This measurement period determines the system response, and is software-controlled to allow both fast and slow measurements with the same system.

During typical operation, the system initially scans the wavelength range of interest to identify the gratings, and then tracks the wavelength of a selected grating.

Calibration: In our first tests the change of the mean AOTF frequency due to applied strain was recorded. To calibrate the system, applied strain was monitored by a conventional strain gauge and a grating mounted next to each other. The system tracked the grating, and a scale factor of $-96.7 \text{ Hz}/\mu\epsilon$ was determined by recording the mean AOTF frequency (Fig. 2).

Similar to many other optical filters, AOTFs are temperature-sensitive. Tracking an unstrained grating held at constant temperature while slowly changing the AOTF temperature, we measured a variation of the mean AOTF frequency of 2.68 kHz/K ; i.e. a 1 K increase in the AOTF temperature results in a signal equivalent to a (compressive) strain of $-27.7 \mu\epsilon$. Therefore the AOTF has to be (i) temperature stabilised, or (ii) temperature-monitored with the PC compensating for any temperature changes. The AOTF temperature may be monitored by a conventional temperature sensor or by interrogating a constant wavelength reference.

The accuracy of the frequency measurement is determined by the accuracy of the measurement period. This period is derived from a quartz, which in the current system has an error of $10^{-9}/\text{sec}$.

System Operation, Experimental Results and Discussions: After scanning the spectrum, the PC displays the recorded data (Fig. 3, top left). The user selects a grating and starts the lock-in mode. An initial fine scan of the chosen grating identifies the points on the slope of the spectrum that will result in the highest sensitivity to wavelength changes (Fig. 3, top right). The system uses the wavelength difference between these points to set the frequency deviation of the FSK in the lock-in mode.

The counter measures the mean AOTF frequency over a measurement period set by the user (Fig. 3, bottom right). The measured frequency is displayed (Fig. 3, middle right) and the frequency change against time may be plotted in real-time. In Fig. 3 the mean AOTF frequency is plotted as its equivalent strain (Fig. 3, bottom left).

The measurement was obtained while tracking grating 1 which was surface-mounted on an aluminium cantilever beam (Fig. 1). Strain was applied by deflecting the beam with a micrometer-driven stage. After an initial measurement with no strain, a strain cycle of $50 \mu\epsilon$, $-50 \mu\epsilon$, and $50 \mu\epsilon$ was applied, before returning to the initial condition. With a measurement period of 100 ms, the trace shows no noise beyond the quantisation noise caused by the limited resolution of the PC display.

Tracking dynamic signals is also possible. Fig. 4 shows the response of grating 2 embedded in a composite cantilever beam and excited by a shaker. The 5 Hz excitation was gradually started and stopped. With a measurement period of 20 ms in this trace, it can be seen that the system noise is similar to the quantisation noise resulting from the display. Identical values of strain were measured with a conventional strain gauge mounted on the surface above the embedded grating.

Multiplexing Schemes: This technique may track the wavelength of multiple gratings due to the large tuning range offered by an AOTF. The current interrogation system shown in Fig. 1 tracks a single grating at any time, but may switch between many. The switching time between gratings is currently 50 ms.

Since the AOTF may be driven by multiple RF frequencies, an extended scheme may interrogate multiple gratings using one feedback loop for each grating [2]. The modulating signals of the different feedback loops should have low crosscorrelation to avoid crosstalk.

Conclusions: We have demonstrated an interrogation system for the tracking of multiple fibre gratings with a convenient frequency output. Static and dynamic changes have been tracked in surface-mounted and embedded gratings. At a measurement period of 100 ms, the standard deviation was equivalent to 0.4 $\mu\epsilon$. The system may operate with transmissive and reflective optical configurations. Gratings at different wavelengths may be either situated along one fibre, or on different fibres as shown in Fig. 1.

Acknowledgements: The authors gratefully acknowledge Westland Aerospace, the U.K. Department of Trade and Industry, and the Engineering and Physical Science Research Council (EPSRC) for supporting this research over the last 2 years; the European Space Agency for funding the initial work; and L. Reekie, J. Tucknott, and L. Dong for supplying the gratings.

References:

- [1] Morey, W.W., Meltz, G., and Glenn, W.H.: 'Fibre optic Bragg grating sensors'. *Proc. SPIE*, 1989, **1169**, pp. 98-107.
- [2] Xu, M. G., Geiger, H., Archambault, J. L., Reekie, L., Dakin, J. P.: 'Novel interrogation system for fibre Bragg grating sensors using an acousto-optic tunable filter', *Electronics Letters*, 1993, **29**, p. 1510f

H. Geiger, M. G. Xu, J. P. Dakin (*Optical Fibre Group, Department of Electronics and Computer Science, University of Southampton, Southampton SO17 1BJ, UK;*
hg@orc.soton.ac.uk)

N. C. Eaton (*Westland Aerospace, East Cowes PO32 6RH, UK*)

List of Figure Captions:

Fig. 1 Block diagram of realised grating interrogation system and experimental setup

Fig. 2 System response to strain applied to a grating (measurement period: 1 sec)

Fig. 3 PC display showing applied static strain (grating 1, measurement period per point: 100 ms)

Fig. 4 Bottom section of PC display showing applied dynamic strain (grating 2, measurement period per point: 20 ms)

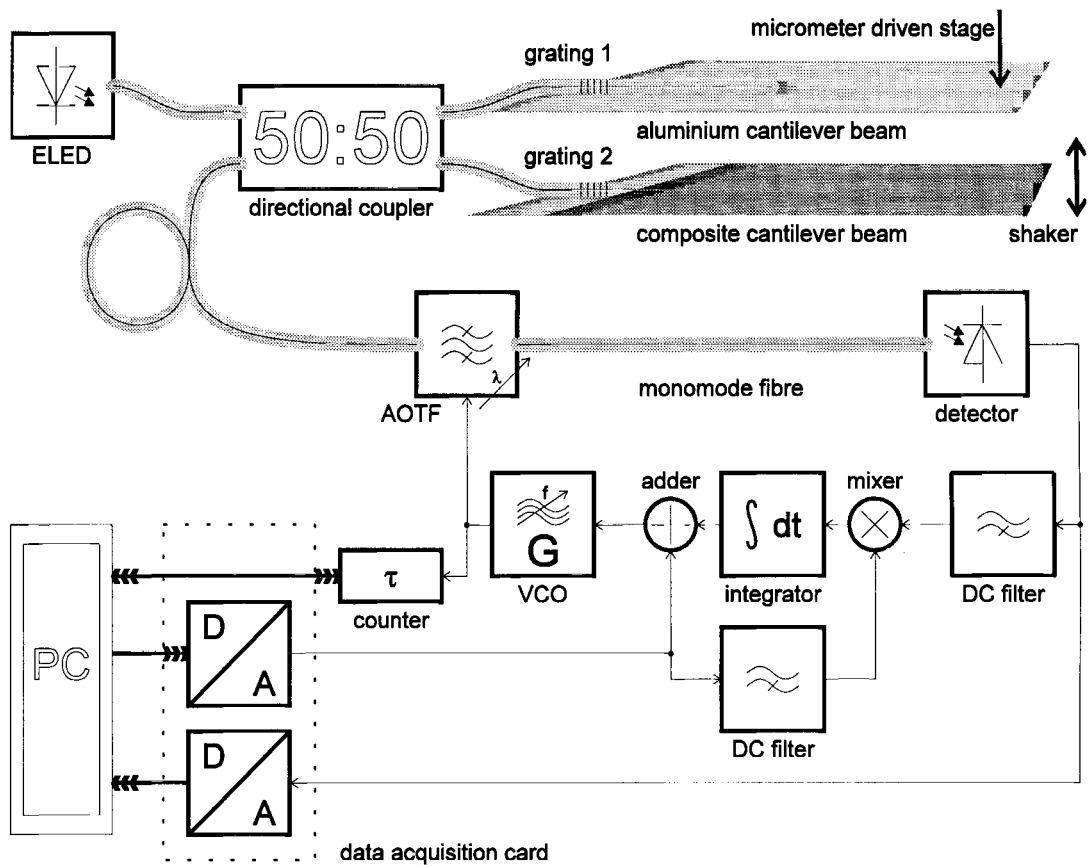


Fig. 1 Block diagram of realised grating interrogation system and experimental setup

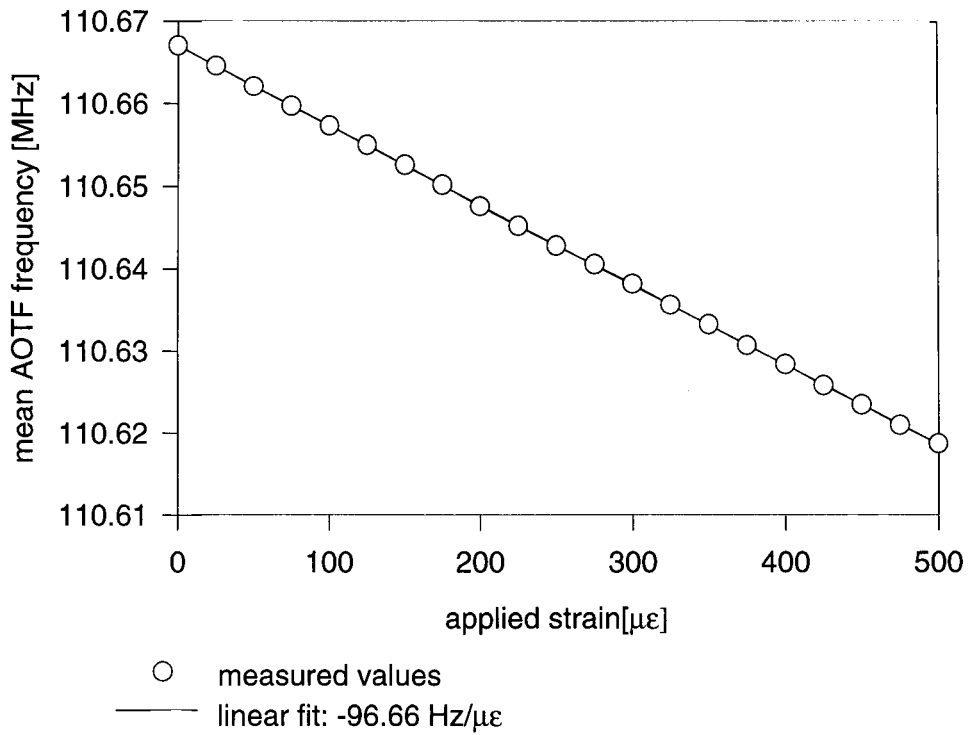


Fig. 2 System response to strain applied to a grating (measurement period: 1 sec)

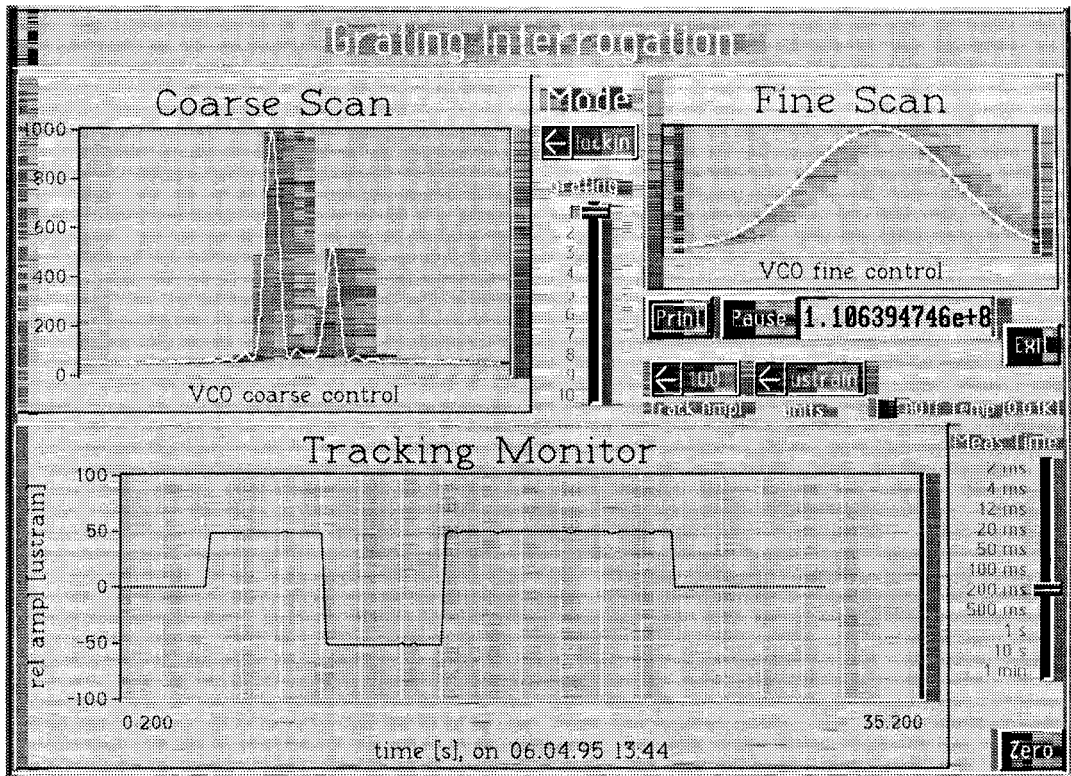


Fig. 3 PC display showing applied static strain (grating 1, measurement period per point: 100 ms)

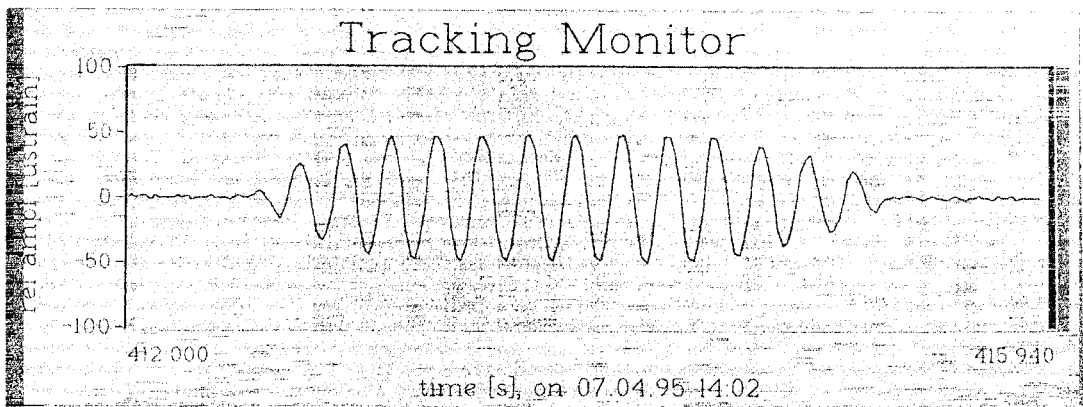


Fig. 4 Bottom section of PC display showing applied dynamic strain (grating 2, measurement period per point: 20 ms)